Journal of Crystal Growth 522 (2019) 191–194

Contents lists available at ScienceDirect

Journal of Crystal Growth

journal homepage: www.elsevier.com/locate/jcrysgro

# Experimental and numerical investigation of laboratory crystal growth furnace for the development of model-based control of CZ process

Kristaps Bergfelds[a,*], Mihails Pudzs[b], Andrejs Sabanskis[a], Janis Virbulis[a]

[a] Department of Physics, University of Latvia, Jelgavas Str. 3, LV-1004 Riga, Latvia
[b] Institute of Electronics and Computer Science, Riga Technical University, Kalku Str. 1, LV-1658 Riga, Latvia

ARTICLE INFO

Communicated by Michail Michailo

*Keywords:*
A1. Computer simulation
A1. Heat transfer
A2. Czochralski method
A2. Growth from melt
B1. Salts
B1. Halides

ABSTRACT

The presented study is focused on laboratory Czochralski crystal growth experiments and their mathematical modelling. The developed small-scale CZ crystal growth furnace is described as well as the involved automation systems: crystal radius detection by image recognition, temperature sensors, adjustable heater power and crystal pull rate. The `CZ-Trans` program is used to model the experimental results – transient, 2D axisymmetric simulation software primarily used for modelling of the industrial-scale silicon crystal growth process. Poor agreement with the experimental results is reached; however, the proven ability to perform affordable, small-scale experiments and successfully model their transient behavior, creates a possibility to develop new process automation solutions in the future.

## 1. Introduction

Mathematical modelling and computer simulations are modern tools which enable the optimization and development of crystal growth processes and their control systems. By using these methods, it is possible to obtain detailed information with high spatial resolution about important physical parameters relevant to the growth process. Some of these parameters are not even available for measurements during the growth process (e.g. thermal stresses, crystallization interface shape, and point-defect distribution) [1]. This information can be used for a model-based control of the actual process, i.e. optimization of crystal growth parameters by using a physical model instead of using conventional signal processing techniques alone.

However, model-based control systems in the crystal growth have been used only in a simplified way. To save computational resources, the precision of developed mathematical models, i.e. the number of solved equations, is significantly reduced [2]. If mathematical models are implemented in their full complexity – using the finite-element method (FEM) with $\approx 10^5$ elements or a similar approach – they are only used for the optimization of the PID control or to calculate process parameter baseline values [3,4] and not for direct, online model-based control.

The authors' research group at the University of Latvia, Department of Physics has developed mathematical modelling tools for transient, 2D axisymmetric simulation of the CZ crystal growth process [5,6] primarily used for modelling of industrial-scale silicon crystals. The developed software (`CZ-Trans`) is proposed as a foundation for a model-based CZ process controller.

However, it is necessary to perform validation of the mathematical model to ensure its relation to an actual crystal growth process by using experiments. As mentioned before, industrial scale experiments are too expensive to be considered as a routine tool for the mathematical model development. Therefore, a small-scale laboratory CZ crystal growth furnace has been built for the purpose of cost-effective validation of the developed mathematical methods and further development of a model-based controller.

## 2. Design of the experimental growth furnace

### 2.1. Furnace description

A laboratory crystal growth furnace with elements required for an automatic control system has been constructed: an optical camera for crystal size measurements, thermocouples for temperature measurements as well as controllers for the pull rate, crystal rotation rate, and heater power (Figs. 1a, b and 2a).

The crucible contains about 150 ml of NaCl-RbCl salt mixture with a molar ratio of 40:60. This composition has eutectic properties which allow for a relatively low melting point of 815 K [7,8]. The growth is performed at pulling speeds around 0.5 mm/min. Crystals can be grown

* Corresponding author.
*E-mail address:* kristaps.bergfelds@lu.lv (K. Bergfelds).

https://doi.org/10.1016/j.jcrysgro.2019.06.029
Received 14 March 2019; Received in revised form 14 May 2019; Accepted 26 June 2019
Available online 29 June 2019

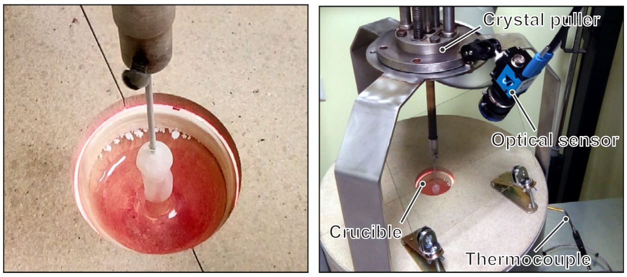


(**a**) Close-up of growth process (**b**) System overview

**Fig. 1.** Photographs of the laboratory CZ crystal growth furnace.

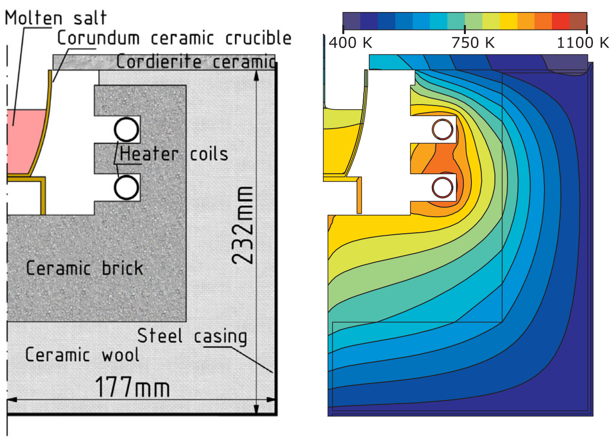


(**a**) Schematics of the furnace construction (**b**) Initial state of the transient simulation (analyzed in Section 3)

**Fig. 2.** Overview of the experimental crystal growth furnace construction as well as the simulated temperature field.

with a diameter about 20 mm.

The low cost of the material, furnace construction and operation allows to perform numerous experiments that will be necessary for the development of the model-based control. Although the model-based controller will most likely be targeted towards silicon CZ growth (CZ-Si) applications, the developed furnace is a cost-effective alternative to industrial CZ-Si experiments.

Although the crystal growth performed with this material first seems considerably different from industrial CZ-Si growth processes (size, temperature range, presence of atmosphere, translucency), the system still exhibits all the physical phenomena that can be related to the silicon crystal growth and does not have the drawbacks associated with some liquid metals e.g. gallium and its eutectics. Namely, the crystal growth can be performed in room conditions and does not require a shielding liquid or a pressure vessel to protect it from the air. Additionally, the temperature field structure in our furnace is similar to the industrial CZ process, contrary to gallium which melts at 30 °C and might require cooling – instead of heating – to be used in crystal growth experiments.

### 2.2. Experimental conditions

The experiment that is further analyzed was performed in the following way:

- The crucible is warmed up with heater coils at 850 W until its content is fully molten. A steel wire is embedded in the melt to act as a seed for the crystal.
- After stable temperature conditions are reached, the heater power is reduced to 750 W to allow the crystallization to occur.

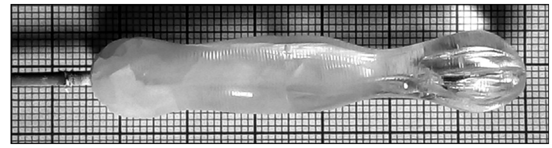

**Fig. 3.** Photograph of the grown crystal.

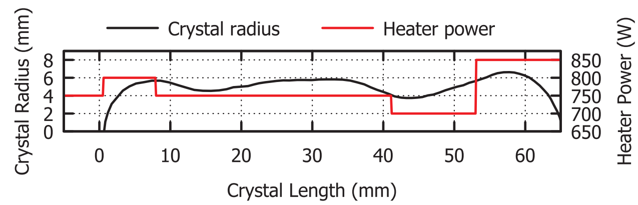


**Fig. 4.** Plot of experimental heater power and resulting crystal radius.

- When the crystal is starting to form, the heater power is again increased to 800 W and the puller is enabled with the velocity of 0.8 mm/min. This corresponds to a crystal length of 0 mm in Fig. 4
- To maintain a stable crystal radius, the power is reduced to 750W. However an additional power drop to 700 W is required to keep the crystal radius above 4 mm.
- Finally, the power is once again raised to 850 W to reduce the crystal radius and detach it from the melt. The grown crystal can be seen in Fig. 3.

The experiment described above, however crude, serves as an excellent basis for the mathematical model validation performed in Section 3. It features simple step-like power adjustments that makes comparison between experiment and simulation easier.

### 2.3. Radius measurement

An essential part of the developed CZ growth system is the ability to detect the size of the crystal being grown. It allows to introduce a feedback loop to the control solutions being tested on this platform. The crystal size detection is performed by the following steps illustrated in Fig. 5.

- (a) An original image is obtained by illuminating the crucible bottom with a laser beam to enhance meniscus visibility. A considerable challenge is to maintain a precise illumination by adjusting the laser beam – high-contrast of the meniscus image is essential to the further steps.
- (b) Image processing (brightness adjustment, noise removal) is performed to obtain a monochrome image with the best possible meniscus contrast.
- (c) A mask is defined with an approximate shape and size of the bright meniscus region. The optimal eccentricity of the mask ellipsis as well as the width of the line must be carefully calibrated to ensure successful recognition.
- (d) A template matching algorithm [9] searches for the highest correlation between the mask and image (the position shown in dark red).
- (e) The size of the mask is adjusted to give the highest correlation. This indicates that the correct crystal size is found.
- (f) As the growth process occurs, the crystal radius signal is registered and processed to remove any artifacts introduced by the imaging system or the uneven growth process causing the crystal to deviate from cylindrical shape.

The proposed method has been implemented by using a freely available, non-commercial software `Python`[10]. This is an important aspect of the small-scale furnace development as the use of commercial

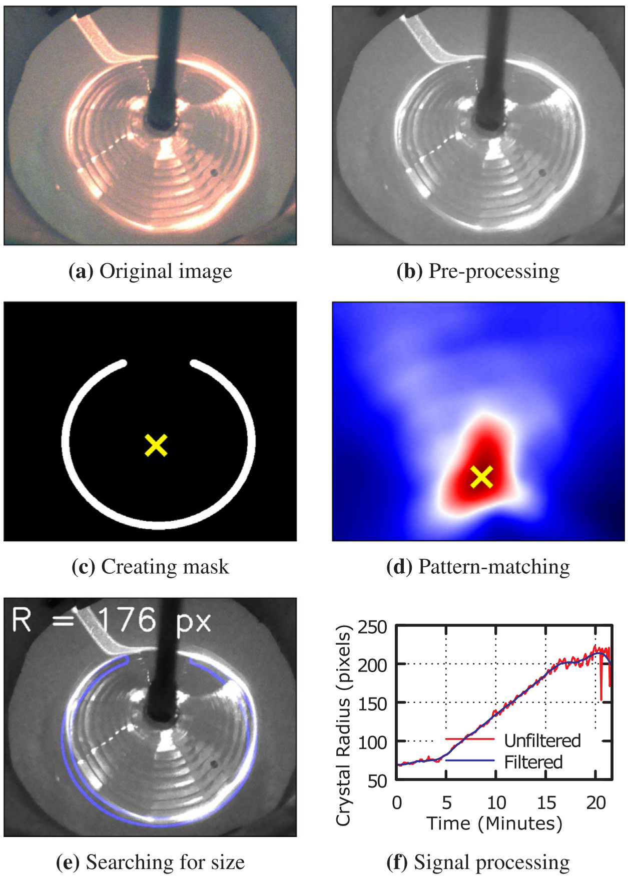


**Fig. 5.** Image processing steps for a successful optical online-detection of the crystal size.

software available on the industrial market would be impractical.

After obtaining the current crystal radius in pixels, a linear calibration function is applied to calculate radius in millimeters. Although this approach does not correct for various effects (an apparent radius change due to a changing meniscus height or dropping melt level), it gives reasonable precision of ± 0.2 mm when comparing with the precise crystal size measured after the experiment.

## 3. Numerical modelling of experiment

### 3.1. Model description

For the studies performed in this article, a previously developed simulation software `CZ-Trans` was used [5]. It can perform axisymmetric non-stationary simulations of the CZ crystal growth process. The following physical phenomena are taken into account: (1) heat transfer by conduction, (2) heat transfer by thermal radiation with view factor approach, shapes of (3) the melt free surface, (4) crystallization interface, and (5) crystal side surface.

To perform simulations with the software, an axisymmetric geometry of the furnace was created with dimensions as shown in Fig. 2. The material properties are listed in Table 1. The melting point of the salt mixture is 815 K [7,8], the latent heat of fusion is 0.202 J/kg [11] and the surface tension is 0.1 N/m [8]. However, the value for the growth angle – i.e. between the melt meniscus and vertical direction required for cylindrical growth – was not found in literature; the value of 0° is currently applied in the model.

The `CZ-Trans` software does not consider radiative heat transfer within the melt and crystal. To accommodate the additional radiative heat losses from the crystallization interface due to the transparency of the crystal, an additional heat flux density is introduced on the crystallization interface. The applied heat flux density is assumed to be lost (radiated) from the crystallization interface and transferred away without absorption and reflection. This method is described in detail and validated in [12].

**Table 1**
Properties of materials shown in Fig. 2. Property notation as follows: $\rho$ – density, $c_p$ – heat capacity, $\lambda$ – thermal conductivity, $\varepsilon$ – emissivity.

| Property<br>Unit | $\rho$<br>$kg/m^3$ | $c_p$<br>J/kg·K | $\lambda$<br>W/m·K | $\varepsilon$<br>– | Ref. |
|---|---|---|---|---|---|
| RbCl-NaCl Melt | 2088 | 680 | 0.80 | 0.70 | [7,8] |
| RbCl-NaCl Crystal | 2800 | 510 | 1 | 0.90 | [7,8] |
| Heater Coils | 7150 | 460 | 100 | 0.70 | [14] |
| Corundum Crucible | 4000 | 1177 | 30 | 0.85 | [11] |
| Ceramic Brick | 575 | 1100 | 0.30 | 0.90 | [15] |
| Ceramic Wool | 320 | 1130 | 0.15 | 0.90 | [16] |
| Cordierite Ceramic | 2600 | 1460 | 3 | 0.80 | [11] |
| Steel Casing | 8000 | 500 | 50 | 0.10 | [11] |

Additionally, 3rd type boundary condition for the temperature field is used on the crystal side surface to model the heat transfer due to convective cooling. The applied heat exchange coefficient is $10\ W/m^2{\cdot}K$ [13].

### 3.2. Initial conditions

The moment when the crystal puller is being enabled (see Section 2.2) was chosen as the first time instance for the transient simulation. These conditions can be replicated in the `CZ-Trans` by setting up a quasi-stationary simulation where a stable outwards growth of the crystal is considered: the growth angle of 60°, the growth velocity on the melt-crystal interface equal to the pull rate of 0.8 mm/min. The temperature field and phase boundaries for the initial state can be seen in Fig. 2b.

### 3.3. Transient simulation results

A transient simulation was performed by applying a heater power distribution that has the same functional shape as in the experiment (Fig. 4). However, the absolute values of the power distribution had to be reduced by a factor of two in order to achieve a crystal shape as observed in the actual growth (Fig. 6). The resulting crystal shape, its temperature field and FEM mesh can be seen in Fig. 7.

## 4. Conclusions

A small-scale laboratory CZ furnace for growing NaCl-RbCl salt crystals has been successfully built. An image recognition software has been developed for online measurements of the crystal size during an experiment. This allows the implementation of automated crystal growth control systems, i.e. future experiments with model-based control.

The calculation software used primarily for the modelling of industrial-scale CZ silicon crystal growth process has been successfully

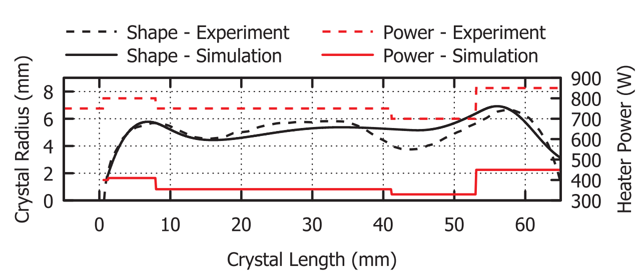


**Fig. 6.** Comparison between simulation and experiment.

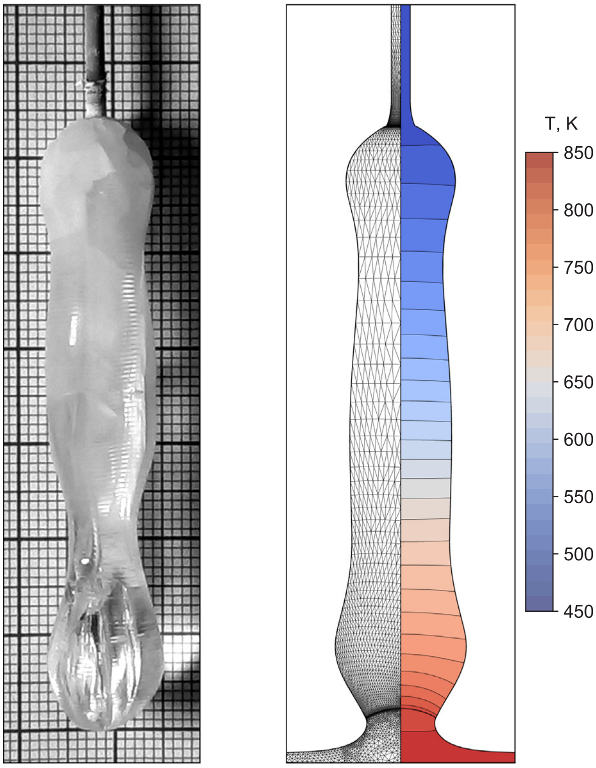


**(a)** Actual crystal **(b)** Simulation result

**Fig. 7.** Comparison between experimental and simulated crystal shapes.

applied to model the laboratory furnace. However, poor match between the simulated and experimental crystal shape and heater power distribution was achieved.

Additional work is necessary to apply the `CZ-Trans` for the built furnace and achieve sufficient precision of modelled parameters. Namely, the third-type boundary conditions of the temperature field must be introduced on the outer surfaces of the furnace geometry; air convection and the created cooling is a considerable effect not present with the industrial CZ equipment where hot furnace parts are located in a vacuum chamber.

The presented simulations show that the applied model has promising applications for the development of a model-based controller for the constructed laboratory furnace.

## Acknowledgements

The present work is carried out at the University of Latvia and has been supported financially by a donation of "Mikrotı̄kls" SIA ("MikroTik" Ltd.), University of Latvia Foundation project *"Implementation of Experimental Laboratory Crystal Growth Furnace"*, project number: 2183.

## References

[1] J. Winkler, M. Neubert, J. Rudolph, A review of the automation of the Czochralski crystal growth process, Acta Phys. Pol. A 124 (2013) 181–192, https://doi.org/10.12693/APhysPolA.124.181 http://przyrbwn.icm.edu.pl/APP/PDF/124/a124z2p03.pdf.

[2] A. Muiznieks, J. Virbulis, A. Lüdge, H. Riemann, N. Werner, Floating zone growth of silicon, in: P. Rudolph (Ed.), Handbook of Crystal Growth, Handbook of Crystal Growth, second ed., Elsevier, Boston, 2015, pp. 241–279, , https://doi.org/10.1016/B978-0-444-63303-3.00007-9 http://www.sciencedirect.com/science/article/pii/B9780444633033000079.

[3] J. Winkler, M. Neubert, J. Rudolph, Nonlinear model-based control of the Czochralski process I: motivation, modeling and feedback controller design, J. Cryst. Growth 312 (2010) 1005–1018, https://doi.org/10.1016/j.jcrysgro.2009.12.074 http://www.sciencedirect.com/science/article/pii/S0022024809011853.

[4] F. Dupret, R. Rolinsky, L. Wu, F. Loix, A. De Potter, N. Van den Bogaert, V. Regnier, Global simulation of CZ and FZ bulk crystal growth: from quasi-dynamic and dynamic modelling to process control and crystal quality optimization, ECS Trans. 18 (2009) 935–943, https://doi.org/10.1149/1.3096557.

[5] A. Sabanskis, K. Bergfelds, A. Muiznieks, T. Schröck, A. Krauze, Crystal shape 2D modeling for transient CZ silicon crystal growth, J. Cryst. Growth 377 (2013) 9–16, https://doi.org/10.1016/j.jcrysgro.2013.04.055 http://www.sciencedirect.com/science/article/pii/S0022024813003242.

[6] A. Sabanskis, K. Bergfelds, J. Virbulis, Transient 2D modelling of Czochralski crystal growth process, Proceedings of the International Scientific Colloquium "Modelling for Electromagnetic Processing", 2014, pp. 87–92.

[7] FactSage, The integrated thermodynamic databank system, 2018. URL http://www.crct.polymtl.ca/fact/documentation/FTsalt/FTsalt_Figs.htm. doi: https://doi.org/10.17616/R3KP9C (accessed: 2019-02-28).

[8] G.J. Janz (Ed.), Molten Salts Handbook, Academic Press, Rensselaer Polytechnic Institute, Troy, New York, 1967, , https://doi.org/10.1016/B978-0-123-95642-2.X5001-1.

[9] O.D. Team, Object detection, 2019. https://docs.opencv.org/2.4/modules/imgproc/doc/object_detection.html (accessed: 2019-05-11).

[10] O.P. Heinisuo, Unofficial pre-built OpenCV packages for Python, 2019. URL https://github.com/skvark/opencv-python (accessed: 2019-05-11).

[11] J. Rumble (Ed.), CRC Handbook of Chemistry and Physics, 99th ed., CRC Press, 2018, http://www.hbcponline.com.

[12] K. Bergfelds, A. Sabanskis, J. Virbulis, Validation of mathematical model for CZ process using small-scale laboratory crystal growth furnace, IOP Conf. Ser. Mater. Sci. Eng. 355 (2018) 012004, https://doi.org/10.1088/1757-899X/355/1/012004 https://iopscience.iop.org/article/10.1088/1757-899X/355/1/012004/meta.

[13] F.P. Incropera, D.P. DeWitt, Introduction to Heat Transfer, sixth ed., John Wiley & Sons, 2011.

[14] Kanthal A: Resistance Heating Alloys for Electric Appliances, Sandvik Group, SE-734 27 Hallstahammar, Sweden, 2018a. URL https://www.kanthal.com/en/products/material-datasheets/wire/resistance-heating-wire-and-resistance-wire/kanthal-a/.

[15] Firebrick 26 Datasheet, Morgan Advanced Materials, 55-57 High Street, Windsor, Berkshire, UK, 2018b. URL http://www.morganthermalceramics.com/en-gb/products/firebrick-and-insulating-firebricks/.

[16] Superwool 607 Bulk Datasheet, Morgan Advanced Materials, 55-57 High Street, Windsor, Berkshire, UK, 2018c. URL http://www.morganthermalceramics.com/media/4720/sw-bulk-data-sheet-english_wme_022018.pdf.